



## Design, development and performance analysis of labyrinth seal in steam turbine application

H.G.PATIL

Research Scholars, Department of Mechanical Engineering, BDCOE  
Sewagram, Dist:-Wardha, Maharashtra – 442001, INDIA.

Dr. V.G. ARAJPURE

Principal, KCES'S college of engineering & Information Technology,  
Jalgaon, Maharashtra – 425002, INDIA.

### ABSTRACT

*Labyrinth seal erosion, roughness, steam path damages, etc are factors that causes steam losses in a steam turbine. Any steam losses occurring locally in HPT, IPT and LPT stages of a steam turbine result in more available steam in losses sealing stages. Recently steam turbine sealing system upgrade in research works has been important. Optimization of steam path design by increased number of sealing strips, use of high pressure aspect ratio and reduced seal root diameter, advanced sealing technology for radial and axial fins, diaphragm packing, optimized labyrinth seal design, robust new seal development are of prime importance. A performance analysis result indicates that the performance value has exceeded the estimated design value.*

**KEYWORDS :** Steam losses, efficiency, seal, performance, thermal stress.

### Introduction

Labyrinth seals have been a subject of research from the early beginnings of steam turbines. As an inherent need of steam turbines gaps must be present between stationary and rotating parts to allow the relative movement. Those gaps open bypass ways which reduce the amount of mass flow rate within the working section of the turbine. Introducing labyrinth seals into these gaps helps to reduce the leakage mass flow, thus increasing the efficiency [28].

The labyrinth seal arrangement at the seal strip consists of an steam inlet. The size of the labyrinth seal can be relatively large in comparison to the seal size and tooth height. This is in order to allow the axial displacement of the rotor due to thermal growth or axial thrust variations. Major effort in research was undertaken to reduce the leakage mass flow rate due to with the help of improved seal design. This study aims at improvising the various characteristic of the labyrinth seals to minimize leakages and is presented geometrically.

### 2. Labyrinth seal design

The labyrinth seal is one of the popular seal designs and is widely used in a variety of steam turbines. As for any seal, the purpose of the labyrinth seal is to reduce the internal steam leakage by increasing the friction to steam flow in the leakage path by dissipating as much of the kinetic energy of the leakage flow as possible. For labyrinth seals, the energy dissipation is achieved by a series of constrictions and cavities. When the steam flows through the constriction (under each tooth), a part of the pressure head is converted into kinetic energy, which is dissipated through small scale turbulence-viscosity interaction in the cavity that follows. This increases the resistance to flow compared to a smooth seal [28].

There are two basic types of labyrinth seal materials configurations: Silicon carbide labyrinth seal and chromium molybdenum labyrinth seal. The main purpose of using a chromium molybdenum labyrinth seal is to provide additional flow resistance. Major operating parameters are the pressure difference (or ratio) between up and down streams of a seal and the size of the clearance that is formed between the seal teeth of one side and the land of the other side. Based on a maximum allowable leakage flow, seal designers decide the seal type, running clearance, and the number of teeth, taking into account other design constraints such as the maximum space for seal installation. Thus, seal design is an optimization process that requires a compromise with designs of other components.

In this work, the steam flow path performances of two typical labyrinth seal types (Silicon carbide labyrinth seal and chromium molybdenum labyrinth seal) were compared. Various thermal analyses were used to predict the flow and leakage performance of the seals. Pre-

dicted leakage behaviors according to clearance size and pressure ratio were compared with experimental data, and leakage performances of the two sealing material types were compared. The effect of the number of teeth was also analyzed. Leakage was predicted using a typical analytic design tool and results were compared with both the experimental data and various thermal analysis results. Essentially, this paper presents a systematic performance comparison between Silicon carbide labyrinth seal and chromium molybdenum labyrinth seal and demonstrates the usefulness of various thermal analyses.

The Labyrinth seal design is used to provide a tortuous passage to help prevent leakage by allowing the steam to pass through a long and difficult gap. Labyrinth seals on rotating shafts provide non contact sealing action by controlling the passage of the steam through a large number of chambers by centrifugal motion as well as by the formation of controlled steam vortices. The steam that escapes from the main chamber gets entrapped in the cavities of labyrinth where it is pressured into a vortex like motion. During the service period of steam turbines, labyrinth seals which are mounted on the rotor, as there is an increase of wear rate in the labyrinth seal material it increases the clearance between the stator & rotor. If the wear rate & clearance is high, it causes the leakage of steam flow through the seals which affects the total efficiency of the steam turbine. The main objective of this work is to evaluate the leakage flow rate due to the clearance caused by the wear of the seal material in labyrinth seals by using CFD and adopting a new material (Silicon Carbide) to the labyrinth seals, thereby calculating the leakage flow rate and compare it with the theoretical calculated leakage flow rate using ANSYS. Apart from this the testing of labyrinth seal during thermal condition is also essential to check its failure. The labyrinth seals are so designed using conventional analytical design [27].

The various dimensions of replaced labyrinth seal are tabulated in which help to take data during design of labyrinth seal and fulfill the requirement.

**Table 1 the various dimension of replaced labyrinth seal of 300 MW in SEC steam turbine model**

Labyrinth seal Data	
Number of teeth	10
Inner diameter	468
Teeth height	6.5
Tooth width[mm]	1
Pitch of teeth[mm]	5
Step height	2
Outer diameter	489

Cutting angle	60
Locking groove width	16
Locking groove depth	1.5

The labyrinth seal design based on ASME steam turbine procedure: The theoretical design calculations are performing using the input parameter such as speed of shaft, inlet pressure, inlet temperature etc.

**2.1 Basic procedure of labyrinth seal**

The design of labyrinth seal is the important step in the completed process of gland sealing design. In order to insure the basic requirement of seal, calculations are carried out for the dimension of seal. This calculation forms an integral part of seal. The basic procedure of the design of seal consists of following step:

**a. Specification of function**

The design of labyrinth seal beginning with the specification of the function of the seal.

**b. Determination of pressure**

In many cases pressure is constructed to determine the pressure acting on the different parts of the seal. The pressure acting on the seal may vary from application to application. The pressure acting on the seal is assumed to be concentrated at some point in the seal or distributed over a particular area.

**c. Selection of material**

The selections of suitable material for the seal depend upon the following four factors:

- a. Pressure acting on the seal area
- b. Clearance of the seal
- c. Thermal expansions
- d. Axial and radial pressure distribution

**d. Failure criteria**

Before finding out dimension of seal it is necessary to know the types of failure by which seal will fail when put in to service. The seal is said to have "failed" when it is unable to perform it is functional satisfactorily.

**e. Determination of Dimensions**

The pressure of the seal depends upon factors viz. the operating condition and mass flow rate steam with temperatures. For example, teeth profile is used for seal because it provides a tortuous passage to help prevent leakage by allowing the steam to pass through a long and difficult gap.

**f. Design Modification**

Revised calculations are carried out for operating condition, margin of safety at critical cross section and thermal stresses taking into consideration the effect of thermal expansion. When these values differ from desired values, the dimensions of the component are modified till desired values are obtained.

**g. Working Drawing**

The last step in the design of labyrinth seal is to prepare a working drawing of the seal showing dimensions.

**h. Analytical Calculations for Labyrinth seal Design**

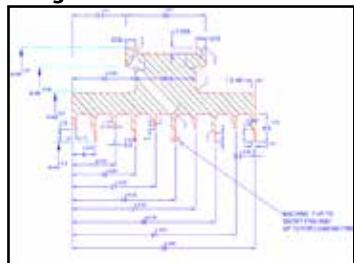


**Figure 1 Labyrinth seal production drawing**

**3. Labyrinth seal manufacturing methods**

Labyrinth seal manufacturing can be done by different techniques available for securing seal. These techniques include:

- 3.1 Forging process
- 3.2 Rough machining (Turning) process
- 3.3 Heat treatment process
- 3.4 Final machining process
- 3.5 Sawing process
- 3.6 Debarring process

**3.1 Forging process**

The process started with melting the steel in the basic electric arc furnace and continued with a vacuum degassing treatment and the pouring of an ingot. Sufficient discard was taken from each ingot to prevent segregation and contamination in the forging material. It is important to avoid segregation due to inclusion in order to achieve uniform mechanical properties of the forging material. The first test specimen was taken during this process in order to have the chemical composition analysis, heat analysis, and product analysis. The ingot was heated to forging temperature according to the forging procedure. The hot-forging process was performed under a press of ample power to adequately work the metal throughout the entire section of the forging. During hot forging, engineers maintained the axial center of the forging in line with the axial center of the ingot. After the forging process was complete, a heat treatment process was applied to prevent cracking and distortion and to accomplish transformation.

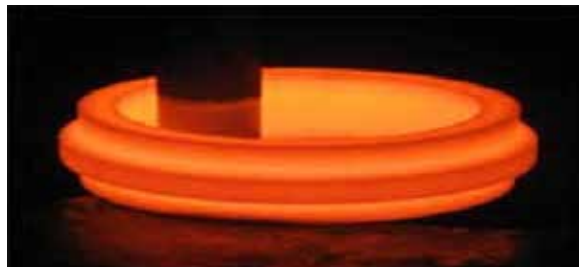


**Figure 2 Labyrinth seal forging ring**

**Phase 1: Normalizing**

During the normalizing, the forging was placed in a horizontal position and cooled in still air. All exterior surfaces of the forging were rough machined before the second phase of the heat treatment.

**Phase 2: Quenching**

During the quenching, the forging was placed in a vertical position and quenched in water.

**Phase 3: Tempering**

During the tempering, the forging remained in a vertical position and cooled in still air.

**Phase 4: Stress relief**

after the heat treatment the forging was stress relieved.

**3.2 Rough machining (Turning) process**

Turning is a form of machining, a material removal process, which is used to create rotational parts by cutting away unwanted material. The turning process requires a rough machining or lathe, forging ring, fixture, and cutting tool. The forging ring is a piece of pre-shaped material that is secured to the fixture, which itself is attached to the Rough machining, and allowed to rotate at high speeds. The cutter is typically a single-point cutting tool that is also secured in the machine, although some operations make use of multi-point tools. The cutting tool feeds into the rotating forging ring and cuts away material in the form of small chips to create the desired shape.



**Figure 3 rough machining of seal ring on lathe machine**  
**Procedure:-**

1. Outer diameter fixture mounted on lathe machine.
2. Turning to be checked and corrected.
3. Gland ring to be fixed or mounted on fixture.
4. Outer cutting tools fixed on tool post after machining started.
5. Facing on outer diameter gland ring.
6. Outer groove cutting started and checked it up to final dimensions.
7. Gland ring removed and further processed for heat treatment.



**Figure 4 rough machining of seal ring completed**

**3.3 Heat treatment process**

After rough machining is completed the gland ring is to be processed for heat treatment for obtaining the desired strength and hardness by using induction heater. Induction heater procedure-

1. Gland ring heated in heater with an increase in temperature 150 c ramp rate per hour up to 750 c.
2. After soaking in 4 hour constant temperature 750 c.
3. Decrease temperature 150 c ramp down rate per hour up to room temperature.
4. After Checking the hardness of gland rings up to 22-25 HRC.

**3.4 Final machining process**

After completion of heat treatment the gland ring is to be process for final machining and the following procedure is carried out.

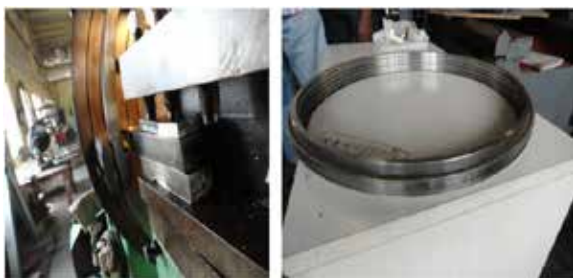


**Figure 5 rough machining of seal ring on lathe machine and other side final ring on table.**

**Sawing process**

Sawing is used for cutting the correct sized segment from a large gland ring. There are several types of saws:-

1. **Band saws-** straight blade ends welded together to make a loop, moving continuously in one direction.
2. **Circular saws-** blade in the shape of a circular disk, rotating continuously.
3. **Abrasive saw-** an abrasive saw also known as a cut off saw or metal chop saw. It is a power tool which is typically used to cut hard materials, such as metal. The abrasive saw generally has a

built in vise or other clamping device and has the cutting wheel and motor mounted on a pivoting arm attached to a fixed base plate. Gland ring cuts the five segments, and one segment is scrap for accurate the dimensions. Shown below is the fig are with a number of segments on tables.



**Figure 6 Numbers of Labyrinth seal segments on tables**

**3.6 Deburring process**

Burrs are sharp edges resulting from cutting and stamping operations. Although usually small in size, burrs can cause assembly problems, interfere with steam flow, and are a common cause of worker injury. Burrs can also cause increased stresses and subsequent fatigue failure of the part. Burr removal, or “deburring,” is a standard practice associated with virtually every segment of the manufacturing process. The vast majority of deburring is performed using mechanical deburring processes, but thermal deburring and electro-chemical deburring processes are also used.



**Figure 7 Deburring process**

**4. Results of performance Analysis**

The outcomes of the performance analysis of **silicon carbide** labyrinth seal and **chromium molybdenum** labyrinth seal for various pressure and mass flow rate, temperature, vibration, turbulence kinetic energy on inlet and outlet, viscosity on inlet and outlet are described here one by one with the help of illustrating the images showing the effect of respective parameters on the labyrinth seal tooth.

**4.1 Results for silicon carbide and chromium molybdenum labyrinth Seal**

In this section the **Mass flow rate average of pressure on inlet** of labyrinth seal is calculated using ANSYS CFD. For this purpose the modeled labyrinth seal to ANSYS CFD is converted as an IGES file and then an automatic mesh is generated. The result of Mass flow rate average of pressure on inlet of labyrinth seal is illustrated in fig.8 having maximum value of chromium molybdenum as 306726 Pa and minimum value of silicon carbide as 160511 Pa. The maximum Mass flow rate average of pressure on inlet lies at the right face of labyrinth seal tooth. The surface location of Mass flow rate average of pressure on inlet can also be seen lying at the face of labyrinth seal tooth in red color shown in figure 8.

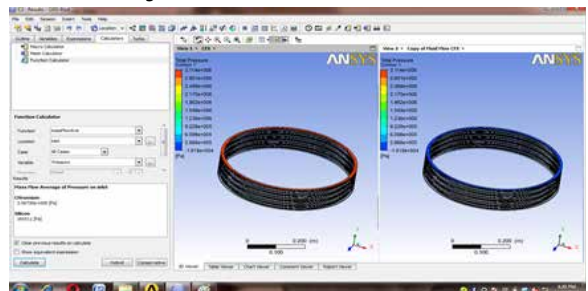


**Figure 8 Mass flow rate average of pressure on inlet**

In this section the **Mass flow rate average of pressure on outlet** of labyrinth seal is calculated using ANSYS CFD. For this purpose the modeled labyrinth seal to ANSYS CFD is converted as an IGES file and then an automatic mesh is generated. The result of Mass flow rate average of pressure on Outlet of labyrinth seal is illustrated in fig. 9 having maximum value of chromium molybdenum as 3091.75 pa and minimum value of silicon carbide as 141.086 Pa. The maximum Mass flow rate average of pressure on Outlet lies at the right face of labyrinth seal tooth. The surface location of Mass flow rate average of pressure on Outlet can also be seen lying at the face of labyrinth seal tooth in red color shown in figure 9.

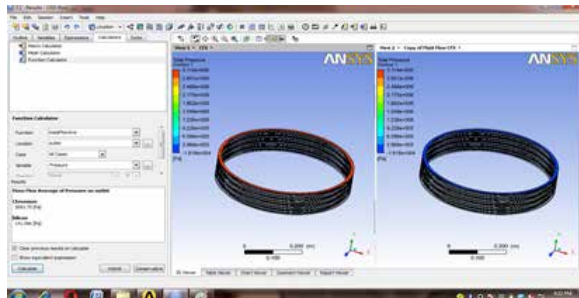


**Figure 9 Mass flow rate average of pressure on outlet**

In this section the **Maximum value of pressure on inlet** of labyrinth seal is calculated using ANSYS CFD. For this purpose the modeled labyrinth seal to ANSYS CFD is converted as an IGES file and then an automatic mesh is generated. The result of Maximum value of pressure on inlet of labyrinth seal is illustrated in fig. 10 having maximum value of chromium molybdenum as 310757.0 Pa and minimum value of silicon carbide as 162269 Pa. The Maximum value of pressure on inlet lies at the right face of labyrinth seal tooth. The surface location of Maximum value of pressure on inlet can also be seen lying at the face of labyrinth seal tooth in red color shown in figure 10.

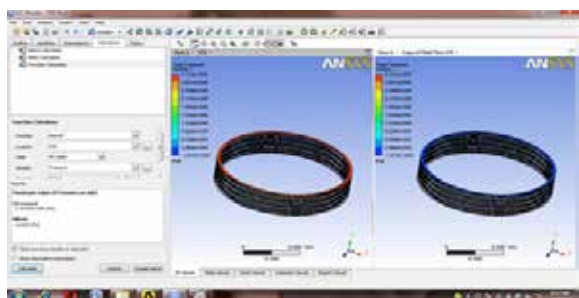


**Figure 10 Maximum value of pressure on inlet**

In this section the **Minimum value of pressure on outlet** of labyrinth seal is calculated using ANSYS CFD. For this purpose the modeled labyrinth seal to ANSYS CFD is converted as an IGES file and then an automatic mesh is generated. The result of Minimum value of pressure on outlet of labyrinth seal is illustrated in fig.11 having maximum value of chromium molybdenum as -13542.9 Pa and minimum value of silicon carbide as -681.89 Pa. The minimum value of pressure on outlet lies at the right face of labyrinth seal tooth. The surface location of minimum value of pressure on outlet can also be seen lying at the face of labyrinth seal tooth in red color shown in figure 11.



**Figure 11 Minimum value of pressure on outlet**

In this section the **Maximum value of turbulence kinetic energy on inlet** of labyrinth seal is calculated using ANSYS CFD. For this purpose the modeled labyrinth seal to ANSYS CFD is converted as an IGES file and then an automatic mesh is generated. The result of Maximum value of turbulence kinetic energy on inlet of labyrinth seal is illustrated in fig. 12 having maximum value of chromium molybdenum as 3956.42 J Kg-1 and minimum value of silicon carbide as 2344.56J Kg-1. The maximum value of turbulence kinetic energy on inlet lies at the right face of labyrinth seal tooth. The surface location of Maximum value of turbulence kinetic energy on inlet can also be seen lying at the face of labyrinth seal tooth in blue color shown in figure 12.

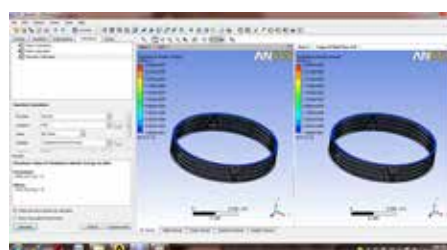


**Figure 12 Maximum value of turbulence kinetic energy on inlet.**

In this section the **Maximum value of temperature inlet** of labyrinth seal is calculated using ANSYS CFD. For this purpose the modeled labyrinth seal to ANSYS CFD is converted as an IGES file and then an automatic mesh is generated. The result of Maximum value of temperature inlet of labyrinth seal is illustrated in fig. 13 having maximum value of chromium molybdenum as 853.152 K and minimum value of silicon carbide as 623.152 K. The Maximum value of temperature inlet lies at the right face of labyrinth seal tooth. The surface location of Maximum value of temperature inlet can also be seen lying at the face of labyrinth seal tooth in red color shown in figure 13.

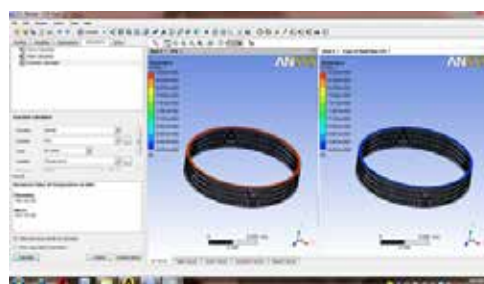


**Figure 13 Maximum value of temperature inlet**

In this section the **Minimum value of velocity on plane** of labyrinth seal is calculated using ANSYS CFD. For this purpose the modeled labyrinth seal to ANSYS CFD is converted as an IGES file and then an automatic mesh is generated. The result of Minimum value of velocity on plane of labyrinth seal is illustrated in fig. 14 having maximum value of chromium molybdenum as 10.9592 M S-1 and minimum value of silicon carbide as 5.96127 M s-1. The Minimum value of velocity on plane lies at the right face of labyrinth seal tooth. The surface location of Minimum value of velocity on plane can also be seen lying at the face of labyrinth seal tooth in blue color shown in figure 14.

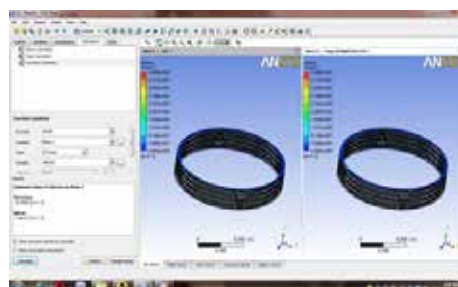


**Figure 14 Minimum value of velocity on plane**

In this section the **Maximum value of velocity on outlet** of labyrinth seal is calculated using ANSYS CFD. For this purpose the modeled labyrinth seal to ANSYS CFD is converted as an IGES file and then an automatic mesh is generated. The result of Maximum value of velocity on outlet of labyrinth seal is illustrated in fig. 15 having maximum value of chromium molybdenum as 420.247 m s<sup>-1</sup> and minimum value of silicon carbide as 402.771 m s<sup>-1</sup>. The Maximum value of velocity on outlet lies at the right face of labyrinth seal tooth. The surface location of Maximum value of velocity on outlet can also be seen lying at the face of labyrinth seal tooth in blue color shown in figure 15.

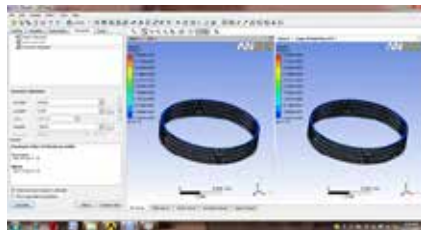


**Figure 15 Maximum value of velocity on outlet.**

In this section the **Maximum value of turbulence eddy dissipation on plane 1** of labyrinth seal is calculated using ANSYS CFD. For this purpose the modeled labyrinth seal to ANSYS CFD is converted as an IGES file and then an automatic mesh is generated. The result of Maximum value of turbulence eddy dissipation on plane 1 of labyrinth seal is illustrated in fig.16 having maximum value of chromium molybdenum as 4.28899 e+009 m<sup>2</sup> s<sup>-3</sup> and minimum value of silicon carbide as 3.49847e+009 m<sup>2</sup> s<sup>-3</sup>. The Maximum value of turbulence eddy dissipation on plane 1 lies at the right face of labyrinth seal tooth. The surface location of Maximum value of turbulence eddy dissipation on plane 1 can also be seen lying at the face of labyrinth seal tooth in blue color shown in figure 16

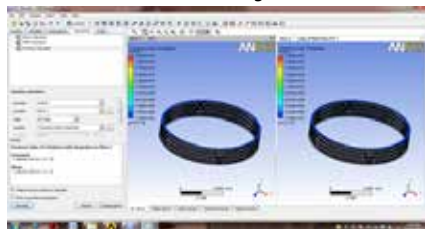


**Figure 16 Maximum value of turbulence eddy dissipation on plane 1**

In this section the **Minimum value of turbulence eddy dissipation on inlet** of labyrinth seal is calculated using ANSYS CFD. For this purpose the modeled labyrinth seal to ANSYS CFD is converted as an IGES file and then an automatic mesh is generated. The result of Minimum value of turbulence eddy dissipation on inlet of labyrinth seal is illustrated in fig. 17 having maximum value of chromium molybdenum as 53827.1 m<sup>2</sup> s<sup>-3</sup> and minimum value of silicon carbide as 22969.6 m<sup>2</sup> s<sup>-3</sup>. The Minimum value of turbulence eddy dissipation on inlet lies at the right face of labyrinth seal tooth. The surface location of Minimum value of turbulence eddy dissipation on inlet can also be seen lying at the face of labyrinth seal tooth in blue color shown in figure 17.

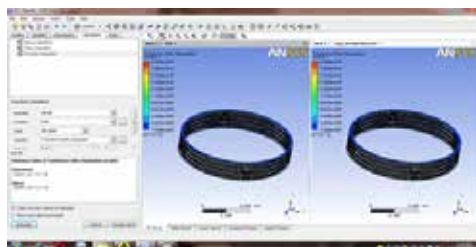


**Figure 17 Minimum value of turbulence eddy dissipation on inlet**

In this section the **Maximum value of eddy viscosity on inlet** of labyrinth seal is calculated using ANSYS CFD. For this purpose the modeled labyrinth seal to ANSYS CFD is converted as an IGES file and then an automatic mesh is generated. The result of Maximum value of eddy viscosity on inlet of labyrinth seal is illustrated in fig. 18 having maximum value of chromium molybdenum as 0.00481085 pa s and minimum value of silicon carbide as 0.000143184 pa s. The Maximum value of eddy viscosity on inlet lies at the right face of labyrinth seal tooth. The surface location of Maximum value of eddy viscosity on inlet can also be seen lying at the face of labyrinth seal tooth in blue color shown in figure 18

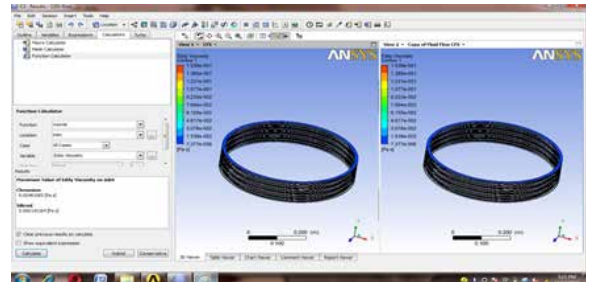


**Figure 18 Maximum value of eddy viscosity on inlet.**

In this section the **Maximum value of eddy viscosity on outlet** of labyrinth seal is calculated using ANSYS CFD. For this purpose the modeled labyrinth seal to ANSYS CFD is converted as an IGES file and then an automatic mesh is generated. The result of Maximum value of eddy viscosity on outlet of labyrinth seal is illustrated in fig. 19 having maximum value of chromium molybdenum as 0.00457105 Pa s and minimum value of silicon carbide as 0.000254972 Pa s. The Maximum value of eddy viscosity on outlet lies at the right face of labyrinth seal tooth. The surface location of Maximum value of eddy viscosity on outlet can also be seen lying at the face of labyrinth seal tooth in blue color shown in figure 19

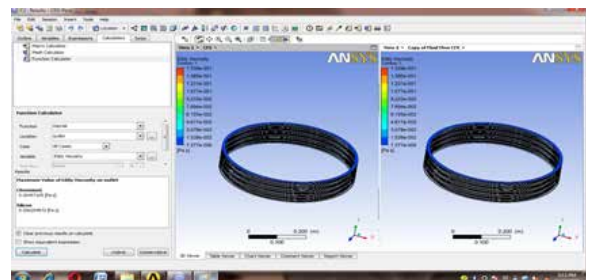


**Figure 19 Maximum value of eddy viscosity on outlet**

In this section the **Minimum value of velocity on inlet** of labyrinth seal is calculated using ANSYS CFD. For this purpose the modeled labyrinth seal to ANSYS CFD is converted as an IGES file and then an automatic mesh is generated. The result of Minimum value of velocity on inlet of labyrinth seal is illustrated in fig.20 having maximum value of chromium molybdenum as 14.5755 m s<sup>-1</sup> and minimum value of silicon carbide as 11.0445 m s<sup>-1</sup>. The Minimum value of velocity on inlet lies at the right face of labyrinth seal tooth. The surface location of Minimum value of velocity on inlet can also be seen lying at the face of labyrinth seal tooth in blue color shown in figure 20

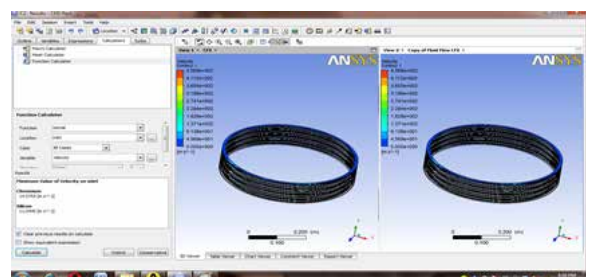


**Figure 20 Minimum value of velocity on inlet**

In this section the **Minimum value of eddy viscosity on plane 1** of labyrinth seal is calculated using ANSYS CFD. For this purpose the modeled labyrinth seal to ANSYS CFD is converted as an IGES file and then an automatic mesh is generated. The result of Minimum value of eddy viscosity on plane 1 of labyrinth seal is illustrated in fig. 21 having maximum value of chromium molybdenum as 3.44806 e -005 Pa and minimum value of silicon carbide as 1.84641 e -005 Pa. The Minimum value of eddy viscosity on plane 1 lies at the right face of labyrinth seal tooth. The surface location of Minimum value of eddy viscosity on plane 1 can also be seen lying at the face of labyrinth seal tooth in blue color shown in figure 21

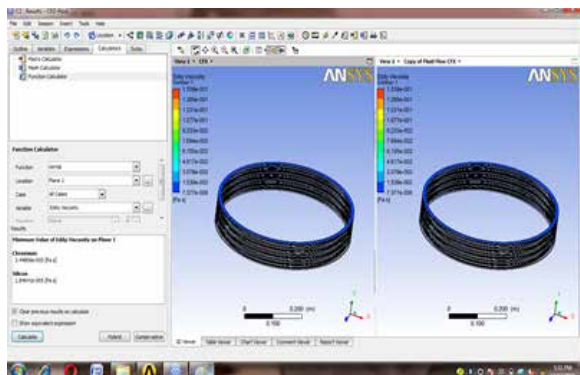


**Figure 21 Minimum value of eddy viscosity on plane 1**

The following table 4.4 shows the comparison of Ansys result between Silicon carbide labyrinth seal and chromium molybdenum labyrinth seal. From the comparative study of total 14 parameters between Silicon carbide labyrinth seal and chromium molybdenum labyrinth seal, it is concluded that the data obtained for Silicon carbide labyrinth seal is comparative less as compared to the chromium molybdenum labyrinth seal.

**4.2 Performance analysis results comparison between chromium molybdenum labyrinth seal and Silicon carbide labyrinth seal.**

Sr. No	Parameters	Chromium molybdenum labyrinth seal	Silicon carbide labyrinth seal
01	Mass flow rate average of pressure on inlet	306726.0	160511
02	Mass flow rate average of pressure on outlet	3091.75	141.086
03	Maximum value of pressure on inlet	310757	162269
04	Minimum value of pressure on outlet	13542.9	681.89
05	Maximum value of turbulence kinetic energy on inlet	3956.42	2344.56
06	Maximum value of temperature inlet	853.152	623.152
07	Minimum value of velocity on plane	10.9592	5.96127
08	Maximum value of velocity on outlet	420.247	402.771
09	Maximum value of turbulence eddy dissipation on plane 1	4.28899	3.49847
10	Minimum value of turbulence eddy dissipation on inlet	53827.1	22969.6
11	Maximum value of eddy viscosity on inlet	0.00481085	0.000143184
12	Maximum value of eddy viscosity on outlet	0.00457105	0.000254972
13	Minimum value of velocity on inlet	14.5755	11.0445
14	Minimum value of eddy viscosity on plane 1	3.44806	1.8464

The above table illustrates the performance analysis comparison between **silicon carbide labyrinth seal and chromium molybdenum labyrinth seal**. The table shows the out-

comes of chromium molybdenum labyrinth seal and Silicon carbide labyrinth seal. The data obtained from analysis help us to understand about the feasibility of Silicon carbide labyrinth seal material in place of chromium molybdenum labyrinth seal and it also clearly shows that values of various parameters and thermal analysis obtained from Ansys CFD for Silicon carbide labyrinth seal are lesser than chromium molybdenum labyrinth seal. Finally it is concluded that Silicon carbide labyrinth seal material hold goods as substitute material for chromium molybdenum labyrinth seal from performance point of view.

**5. Conclusions**

In this paper, we have described the application of labyrinth seals to steam turbines, covering the benefits in performance and the design issues that must be considered. To steam turbines running with a combination of interstage packing, end packing, and bucket tip seals. Labyrinth seals installed more recently in a utility steam turbine have also been inspected and were found to be in excellent condition with the exception of one gland tip seal subjected to a particularly abusive operating environment. While gland tip seals are still under development, steam turbine shaft labyrinth seals are now a robust product offering from the OEM with validated leakage reduction and reliability performance. Development efforts continue both to refine the current design and to expand the range of possible applications. This paper discusses the performance benefits of the labyrinth seal and the design considerations important to a robust design in a steam turbine. Improved seal performance offers substantial opportunities for turbine performance as reduced leakages lead to greater efficiency and power output, and tighter control of turbine flows. There are a number of seal locations on a steam turbine that have significant performance. These include the interstage shaft packing, the end packing, and the bucket tip seals. Performance analysis shows the outcomes of chromium molybdenum labyrinth seal and Silicon carbide labyrinth seal. The data obtained from analysis help us to understand about the feasibility of Silicon carbide labyrinth seal material in place of chromium molybdenum labyrinth seal and it also clearly shows that values of various parameters and thermal analysis obtained from Ansys CFD for Silicon carbide labyrinth seal are lesser than chromium molybdenum labyrinth seal. Finally it is concluded that Silicon carbide labyrinth seal material holds good as substitute material for chromium molybdenum labyrinth seal from performance point of view.

**REFERENCES**

1. A.I. Golubev, L.A. Kondakov, V.B. Ovander, V.V. Gordeev, B.A. Furmanov and B.V. Kargin. "Seals and sealing equipment", Moscow, Mechanical Engineering, 1994.
2. A.I. Belousov, S.V. Falaleev, A.S. Vinogradov and P.V. Bondarchuk. "Problems of application of face gasdynamic seals in aircraft engines". Russian Aeronautics, vol.50 (4), pp. 390-394, 2007. doi: 10.3103/S1068799807040083
3. A. Stodola and P. Smith. "Steam and Gas Turbines (translated by Loewenstein, L. C.)", vol. 1, New York, 1945.
4. H. M. Martin, "Labyrinth Packings". Engineering, pp. 35-36, 1908.
5. B. Hodgkinson. "Estimation of the Leakage through a Labyrinth Gland". Proceedings of the Institution of Mechanical Engineers, vol.141, pp. 283-288, 1939.
6. A. Egli. "The Leakage of Steam through Labyrinth Seals". Transactions of the ASME, pp. 115-122, 1935.
7. H.L. Stocker, D.M. Cox and G.F. Holle, "Aero-dynamic Performance of Conventional and Advanced Design Labyrinth Seals with Solid-Smooth". Abradable and Honeycomb Lands. NASA-CR-135307, 1977.
8. V. Schramm, fluence K. Willenborg, ofa S. Kim and S. Wittig. "In Honeycomb-Facing on the Flow through a Stepped Labyrinth Seal". ASME Paper 2000- GT-0291, 2000
9. H. Zimmermann, A. Kammerer and K.H. Wolff. "Performance of Worn Labyrinth Seals". ASME Paper No. 94-GT-131, 1994.
10. B.H. Song and S.J. Song. "Lateral forces from single gland rotor labyrinth seals in turbines". ASME Turbo Expo 2002, GT-2002-30335, 2002.
11. A.M. Gamaland J.M. Vance. "Labyrinth seal leakage tests: tooth profile, tooth thickness, and eccentricity effects". ASME Turbo Expo 2007, GT2007-27223, 2007.
12. H. Zimmermann and K.H. Wolff. "Air System Correlations: Part 1-Labyrinth Seals". ASME Paper 98-GT-206.
13. H.L. Stocker, D.M. Cox and G.F. Holle. "Aero-dynamic Performance of Conventional and Advanced Design Labyrinth Seals with Solid-Smooth". Abradable and Honeycomb Lands. NASA-CR-135307, 1998.
14. P.A.E. Steward and K.A. Brasnett. "The Contribution of X-Ray to Gas Turbine Air Sealing Technology". AGARD-CP-237, 10.1-10.13, 1978.
15. K.N. Chaadaev and D.K. Novikov. "Dynamics of a rigid rotor in the NK-14ST-10 engine free power turbine with sliding bearings". Russian Aeronautics, vol.52 (4), pp. 426-431, 2009.
16. S. Falaleev, A. Vinogradov and P. Bondarchuk. "Influence research of extreme operates

- conditions on the face gas dynamic seal characteristics". Technische Akademie Esslingen International Tribology Colloquium Proceedings, vol.15, p. 208, 2006.
18. Y. Muller, "Secondary air system model for integrated thermo mechanical analysis of a jet engine". Proceedings of ASME Turbo Expo 2008: Power for Land, Sea and Air, GT2008-50078, 2008.
  19. A. Peschiulli, D. Coutandin, M. Del Cioppo and M. Damasio. "Development of a numerical procedure for integrated multidisciplinary thermal-steam-structural analysis of an aero engine turbine". ASME Turbo Expo 2009, GT2009-59875, 2009.
  20. Y. Wang, C. Young, G. Snowsill and T. Scanlon. "Study of Airflow Features through Step Seals in the Presence of Disengagement due to Axial Movement", ASME Turbo Expo 2004, GT2004-53056, 2004.
  21. A.I. Belousov, S.V. Falaleev and A.S. Demura. On application of the theory of face seals with microgrooves to high-speed FV engine rotors. Russian Aeronautics, vol.52 (3), pp. 335-339. doi: 10.3103/S106879980903012X, 2009.
  22. A.S. Vinogradov. "Seal design features for systems and units of aviation engines". Life Science Journal, vol.11(8), pp. 575-580, 2014.
  23. S.V. Falaleev. "Hydrodynamic characteristics of the face seal taking into account lubricant film breakdown, inertial forces and complex clearance form". Life Science Journal, vol.11(9), pp. 337-343, 2014.
  24. I.B. Celik, U. Ghia and P.J. Roache. "Procedure for Estimation and Reporting of Uncertainty Due to Discretization in CFD Applications". Journal of Steams Engineering, 2008.
  25. I. Zhdanov, S. Staudacher and S. Falaleev. "An advanced usage of meanline loss systems for axial turbine design optimisation". Proceedings of the ASME Turbo Expo 6 A. doi: 10.1115/GT2013-94323, 2013.
  26. N.T. Tikhonov and V.N. Matveev. "Experimental study of influence of upper and lower overlap magnitudes on efficiency of radial centripetal micro turbines with shrouded rotor". Soviet Aeronautics, vol.30 (4), pp. 120-123, 1987.
  27. S.K. Bochkarev, A.Ya. Dmitriev, V.V. Kulagin, S.V. Makeenko, V.V. Mosoulin and A.A. Mossoulin, "Experience and problems of computer aided thermogasdynamic analysis of testing results for gas-turbine engines with complex schemes". Izvestiya Vysshikh Uchebnykh Zavedenij. Aviatcionnaya Tekhnika, vol.2, pp. 68-70, 1993.
  28. L. K. Chakravarthy Dr. P. Srikanth, 2013, "Modeling and analysis of labyrinth seal used in steam turbines", IJSR, ISSN 2319-7064, Page 1808-1813.
  29. Axel PFAU, "Loss Mechanism in Labyrinth seals of Shrouded Axial turbines", 2003, page 1-185.